MOLECULAR AND CELLULAR BIOLOGY, Aug. 2002, p. 5813–5825 Vol. 22, No. 16
0270-7306/02/$04.00+0 DOI: 10.1128/MCB.22.16.5813–5825.2002

The Zinc Finger Domain of NEMO Is Selectively Required for NF-κB Activation by UV Radiation and Topoisomerase Inhibitors

Tony T. Huang,[1] Shelby L. Feinberg,[2] Sainath Suryanarayanan,[1] and Shigeki Miyamoto[1,2]*

Programs in Molecular and Cellular Pharmacology[1] and Cellular and Molecular Biology,[2] Department of Pharmacology, University of Wisconsin—Madison, Madison, Wisconsin 53706-1532

Received 8 March 2002/Returned for modification 15 April 2002/Accepted 10 May 2002

Exposure of mammalian cells to UV radiation was proposed to stimulate the transcription factor NF-κB by a unique mechanism. Typically, rapid and strong inducers of NF-κB, such as tumor necrosis factor alpha (TNF-α) and bacterial lipopolysaccharide (LPS), lead to rapid phosphorylation and proteasomal degradation of its inhibitory protein, IκBα. In contrast, UV, a relatively slower and weaker inducer of NF-κB, was suggested not to require phosphorylation of IκBα for its targeted degradation by the proteasome. We now provide evidence to account for this peculiar degradation process of IκBα. The phospho-IκBα generated by UV is only detectable by expressing a ΔF-box mutant of the ubiquitin ligase β-TrCP, which serves as a specific substrate trap for serine 32 and 36 phosphorylated IκBα. In agreement with this finding, we also find that the IκB kinase (IKK) phospho-acceptor sites on IκBα, core components of the IKK signalsome, and IKK catalytic activity are all required for UV signaling. Furthermore, deletion and point mutation analyses reveal that both the amino-terminal IKK-binding and the carboxy-terminal putative zinc finger domains of NEMO (IKKγ) are critical for UV-induced NF-κB activation. Interestingly, the zinc finger domain is also required for NF-κB activation by two other slow and weak inducers, camptothecin and etoposide. In contrast, the zinc finger module is largely dispensable for NF-κB activation by the rapid and strong inducers LPS and TNF-α. Thus, we suggest that the zinc finger domain of NEMO likely represents a point of convergence for signaling pathways initiated by slow and weak NF-κB-activating conditions.

Exposure of mammalian cells to short-wavelength UV radiation stimulates signaling pathways that activate transcription factors, which elicit various biological responses through their induction of target genes. One of the most studied groups of transcription factors induced by UV radiation are members of the NF-κB/Rel family. The NF-κB/Rel family of transcription factors regulates the expression of genes critical for multiple biological processes, including inflammatory reactions, immune responses, and apoptosis (9, 40). NF-κB is normally kept inactive in the cytoplasm of unstimulated cells and consequently must be translocated into the nucleus to function. The subcellular localization of NF-κB is tightly controlled by a family of inhibitory proteins called IκBs, the most prominent and well-studied being IκBα (11, 12, 23, 29, 38). Nuclear uptake of NF-κB is prevented upon its tight association with IκBα. Exposure of cells to a variety of extracellular stimuli, such as tumor necrosis factor alpha (TNF-α), interleukin-1 (IL-1), or lipopolysaccharide (LPS) leads to the rapid phosphorylation, ubiquitination, and ultimately proteasome-mediated degradation of IκBα, which releases NF-κB and allows it to translocate into the nucleus to regulate gene transcription (18).

The mechanisms of IκBα degradation by many rapid and strong inducers of NF-κB, such as TNF-α, IL-1, and LPS, have been well characterized due to the relative ease of capturing the phosphorylated and multiubiquitinated intermediates of IκBα prior to its degradation. However, the same cannot be said for deciphering the mechanism involved in IκBα proteolysis by slow- and weak-activating NF-κB stimuli such as UV and other genotoxic stress inducers, including the topoisomerase poisons camptothecin (CPT) and etoposide (VP16) (18). In particular, recent studies have purported the UV-induced NF-κB signaling pathway to be exceptional (1, 21). There are three points of contention that hold the UV signaling mechanism distinct from the "fast-kinetic" and strong NF-κB-inducing mechanism. First, UV irradiation induces the degradation of IκBα and activation of NF-κB with slower kinetics, with activity peaking by 2 to 4 h after treatment. This is compared to TNF-α or IL-1, whose inducible NF-κB activity peaks within 10 to 20 min at much higher levels, as measured by both NF-κB DNA-binding and transient reporter assays and IκBα degradation by Western blotting (1). Second, in contrast to the fast and strong inducers, IκB kinase (IKK) activity is undetectable in response to UV irradiation. Consistent with this observation, the inducible degradation of IκBα was unaffected by mutations at the IKK phospho-acceptor sites or by transient overexpression of dominant-negative IKK mutants (1, 21). Third, unlike fast and strong inducers, UV irradiation does not accumulate the phospho-intermediate of IκBα (pIκBα), even in the presence of potent proteasome inhibitors such as *N*-acetyl-leucinyl-leucinyl-norleucinal (AcLLnL) or lactacystin (21).

The multisubunit IKK complex is responsible for the inducible phosphorylation of IκBα, and it is likely the point of convergence for most NF-κB-activating stimuli (14, 18, 35). The core components of IKK contain two catalytic subunits, IKKα/IKK1 and IKKβ/IKK2, and an important regulatory protein, NEMO (also named IKKγ) (18). How diverse signals converge on the IKK complex is not yet known. However,

* Corresponding author. Mailing address: Department of Pharmacology, University of Wisconsin—Madison, 3795 Medical Sciences Center, 1300 University Ave., Madison, WI 53706-1532. Phone: (608) 262-9281. Fax: (608) 262-1257. E-mail: smiyamot@facstaff.wisc.edu.

NEMO knockout mouse embryonic fibroblasts (MEFs) and a pre-B cell line derivative, 1.3E2, that is deficient for NEMO expression are completely defective in cytokine- and LPS-induced activation of IKK and subsequently, the activation of NF-κB (32, 34, 44). The interaction between NEMO and IKKα/IKKβ complexes also proves to be critical for proinflammatory activation of IKK, since disrupting this interaction with a cell-permeable inhibitory peptide reduces signal-dependent NF-κB activity (24). The activation of the IKK complex leads to the rapid phosphorylation of serine-32 and serine-36 of IκBα (4, 7, 26, 43, 47). The pIκBα substrate is then recruited to the ubiquitin machinery through a specific and direct interaction with the F-box/WD E3 ubiquitin ligase β-TrCP (8, 10, 20, 36, 37, 42, 45). The F-box domain of β-TrCP plays an essential role in the ubiquitination process through recruitment of other components of the SCF complex that serve as crucial adaptors for bringing an E2 (ubiquitin-conjugating enzyme) to the substrate (18). It has been shown that an F-box deletion mutant of β-TrCP can bind pIκBα better than the original protein (36).

In the present study, we used an F-box deletion mutant of β-TrCP as a tool to capture pIκBα intermediates that are produced at low levels in cells exposed to UV and other slow-kinetic and weak inducers of NF-κB activity. We also employed IKK chemical inhibitors, IKKβ dominant-negative mutants, stable transfection, and complementation studies of NEMO-deficient cell lines in order to uncover an important and necessary role for the IKK complex in the regulation of the UV-induced NF-κB signaling pathway. Our study provides evidence that slow kinetics and weak activators of NF-κB, including UV irradiation, require the NEMO zinc finger domain to activate NF-κB. Interestingly, fast-kinetic and strong activators of NF-κB, such as LPS and TNF-α, can still activate NF-κB efficiently in the absence of this NEMO C-terminal region. Our findings suggest that the zinc finger domain of NEMO likely represents a point of convergence for signaling pathways initiated by slow and weak NF-κB-activating conditions.

MATERIALS AND METHODS

Reagents and antibodies. The peak emission wavelength of the UV-C lamp (Fisher Biotech UV Cross-Linker) used was 254 nm. CPT, VP16, dimethyl sulfoxide (DMSO), Bay-11-7082, and bacterial LPS were purchased from Sigma. Stock solutions were prepared in DMSO at 10 mM (CPT), 10 mM (VP16), and 50 mM (Bay-11-7082). LPS was prepared in RPMI growth medium at 1 or 10 mg/ml. Human recombinant TNF-α, MG132, AcLLnL, and z-VAD were purchased from CalBiochem and resuspended in phosphate-buffered saline (PBS) containing 0.1% bovine serum albumin (fraction V; Sigma) and DMSO, respectively. In each experiment, all samples received the same amounts of DMSO to control for potential DMSO effects. All stock solutions were stored in aliquots at either −70°C or −20°C. Immunoglobulin G antibodies to IKKα (M280), NEMO (FL-419), c-Myc (9E10), IκBα (C-21), IKKα/IKKβ (H-470), p65 (C-20-G), and glutathione *S*-transferase (GST) (B-14) were purchased from Santa Cruz Biotechnology. A monoclonal anti-Flag antibody was purchased from Sigma. A monoclonal anti-HA.11 (influenza virus hemagglutinin [HA] epitope) antibody was purchased from Covance. Horseradish peroxidase-conjugated anti-rabbit and anti-mouse antibodies were obtained from Amersham Pharmacia Biotech. Cell preparations and extracts were made with the total cell extract buffer (20 mM HEPES [pH 7.9], 350 mM NaCl, 20% glycerol, 1% NP-40, 1 mM $MgCl_2$, 0.5 mM EDTA, 0.1 mM EGTA, 0.5 mM dithiothreitol [DTT], 0.5 mM phenylmethylsulfonyl fluoride [PMSF], 1 μg of aprotinin per ml) and used for both Western blot analysis and electrophoretic mobility shift assay (EMSA). The Igκ-κB oligonucleotide probe and conditions for EMSA were previously described (27). Western immunoblots were performed as described previously (27) and developed by using an enhanced chemiluminescence procedure according to the manufacturer (Amersham Pharmacia Biotech). Blots were then exposed to X-ray film (Kodak).

Cell culture. 70Z/3, 70Z/3-CD14, and 1.3E2 murine pre-B cells were maintained in RPMI 1640 medium (Cellgro; Mediatech) supplemented with 10% fetal bovine serum (HyClone Laboratory, Inc.), 0.05 mM β-mercaptoethanol, 1,250 U of penicillin G (Sigma), and 0.5 mg of streptomycin sulfate (Sigma) per ml in a 5% CO_2 humidified incubator (Forma). MEFs, human cervical carcinoma (HeLa) cells, and human embryonic kidney 293 (HEK293) cells were maintained in 10% fetal bovine serum and antibiotics as described above in a 10% CO_2 incubator. Tissue culture plates were 0.1% (wt/vol) gelatin-coated for HEK293 cells. HEK293 cells were transiently transfected by using a standard calcium phosphate precipitation method (2).

Luciferase reporter assay. Wild-type and IKK double-knockout (DKO) MEF lines (generous gifts from I. Verma) were transfected with 50 ng of 3xκB-Luc and 200 ng of CMV–β-Gal vectors by using the Effectene (Qiagen) transfection reagent. At 36 h after initial transfection, cells were either untreated or treated with TNF-α (10 ng/ml) or exposed to UV-C (60 J/m^2) for an additional 8 h. The cell extract preparation and luciferase assay were performed according to the instructions in the luciferase kit from Promega. β-Galactosidase activity was measured by using the Galacton-Plus kit purchased from Tropix (Bedford, Mass.). The transfection efficiency was normalized within each cell line with β-galactosidase activity. All transfection experiments were done in triplicate and were repeated three times.

Construction of NEMO mutants. Human wild-type NEMO N terminally fused to six tandem Myc tags was cloned into the pcDNA3 vector (Invitrogen) at *Eco*RI/*Xba*I sites (gift from Z. Chen). Truncation and point mutations in NEMO were made by PCR mutagenesis. To make the N-terminal 120-amino-acid truncation mutant of NEMO, a forward primer containing an *Eco*RI engineered site flanking the start site at amino acid 121 was designed (5′-GAAGAATTCCGC TCTGCGGGAGGTGGAGCAC-3′). To make C-terminal 25-amino-acid truncation mutant, the same strategy was employed. The reverse primer was designed containing a flanking *Xba*I site, followed by a termination codon immediately after amino acid 394 of NEMO (5′-GAATCTAGACTAGTCAGGTGGCTCC TCGGGG-3′). For the construction of NEMO zinc finger point mutations, reverse primers were made covering the entire zinc finger domain with a flanking *Xba*I site except that either (i) codon 417 was changed from cysteine to arginine or alanine or (ii) codon 406 was changed from asparate to valine. The forward primer to PCR-amplify the C-terminal NEMO mutants contains a flanking *Eco*RI site (5′-GAAGAATTCCATGAATAGGCACCTCTGGAAG-3′).

Generation of stable transfectants in cells. 1.3E2 cells were reconstituted with 6× Myc-tagged NEMO wild-type and mutant constructs by electroporation or retroviral infection methods as described previously (27). For electroporation, briefly, 2×10^7 cells were washed once with culture media and then resuspended in 750 μl of media with 20% fetal bovine serum and transferred directly to a 0.4-cm electrode gap Gene Pulser cuvette (Bio-Rad). Then, 40 μg of expression DNA plasmid was preincubated with the cells on ice for 10 min. Cells were then electroporated at 240 V and 950 μF in a Gene Pulser apparatus with capacitance extender (Bio-Rad). After the pulse, cells were incubated on ice for 5 min, resuspended in culture media and placed in the 37°C incubator. After 24 h of incubation, 1 mg of G418 (Mediatech)/ml was added to select for resistant pools. Dead cells were removed by using lymphocyte separation medium (Mediatech).

Kinase assay and immunoprecipitation. A total of 2×10^6 cells were treated as indicated. Pellets were lysed in 10% PBS and 90% lysis buffer (20 mM Tris [pH 7.0], 250 mM NaCl, 3 mM EDTA, 3 mM EGTA, 0.5% NP-40, 2 mM DTT, 0.5 mM PMSF, 20 mM β-glycerol phosphate, 1 mM sodium orthovanadate, 1 μg of leupeptin/ml, 1 μg of aprotinin/ml, 10 mM *p*-nitrophenyl phosphate [PNPP], 10 mM sodium fluoride). Supernatants were diluted further in lysis buffer, and 1 μg of α-IKKα antibody (M-280; Santa Cruz Biotechnology) was added to each tube. Samples were rotated for 60 min at 4°C. Protein G-Sepharose beads (Amersham Pharmacia Biotech) were then added to each tube, and the samples were rotated for 90 min at 4°C. Afterward, samples were washed four times in lysis buffer and two times in kinase buffer (20 mM HEPES [pH 7.7], 2 mM $MgCl_2$, 2 mM $MnCl_2$, 1 mM DTT, 0.5 mM PMSF, 10 mM β-glycerol phosphate, 300 μM sodium orthovanadate, 1 μg of leupeptin/ml, 1 μg of aprotinin/ml, 10 mM PNPP, 10 mM sodium fluoride, 10 μM ATP). The IKK kinase activity was assayed for in the kinase buffer with 1 μg of substrate (GST-IκBα1-66) and 1 μCi of [γ-^{32}P]ATP for 60 min at 30°C. Glutathione-Sepharose beads (Amersham Pharmacia Biotech) and excess kinase buffer were added to each reaction mix. These samples were tumbled for 60 min at 4°C. The buffer was removed, and the beads were washed once in kinase buffer. The samples were boiled in 2× sodium dodecyl sulfate (SDS) leading buffer, and the proteins were separated by SDS-polyacrylamide gel electrophoresis (PAGE). Proteins were then transferred to polyvinylidene difluoride membranes and exposed to autoradiography. The membranes were subjected to Western blotting with the

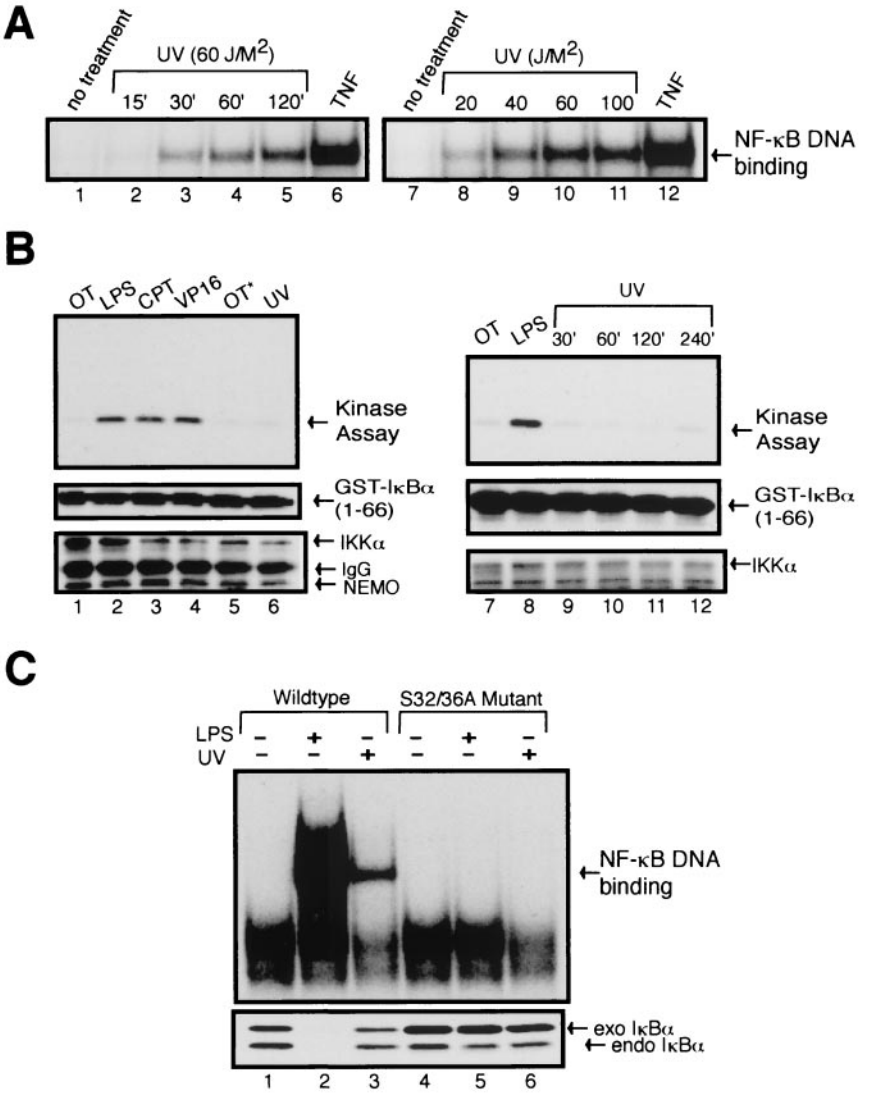

FIG. 1. Stably expressed S32/36A mutant of IκBα inhibits UV-induced NF-κB DNA-binding activity. (A) HeLa cells were either untreated or exposed to UV (60 J/m^2) for the indicated time periods (lanes 2 to 5) or exposed to indicated doses of UV for 2 h (lanes 8 to 11) or treated with TNF-α (10 ng/ml) for 15 min for the control. Total cell extracts were prepared and NF-κB DNA-binding activity was determined by EMSA. (B) 70Z/3 cells were either untreated, treated with LPS (10 μg/ml) for 30 min, treated with CPT (10 μM) or VP16 (10 μM), or exposed to UV (60 J/m^2) for 2 h (lane 6) or at the indicated time points (lanes 9 to 12). An asterisk indicates the handling of cells similar to that of UV-treated cells (lane 5). Whole-cell lysates were prepared, and IKK activity was measured by the immunecomplex kinase assay (upper panels) (see Materials and Methods). The levels of IKKα, GST-IκBα, and NEMO were determined by immunobloting with antibodies specific to IKKα, GST, and NEMO (lower panels). (C) 70Z/3-CD14 cells were stably transfected by a retroviral infection method with either HA-tagged wild-type or S32/36A mutant mouse IκBα. Stable clones from both wild-type and mutant-expressing pools of cells were picked and analyzed. Total cell extracts from the samples were analyzed by EMSA (upper panel) and Western blotting with anti-IκBα antibody (lower panel). Prior to the treatment conditions, the cells were pretreated with z-VAD (25 μM) for 30 min to prevent caspase-dependent cleavage of IκBα (see Discussion). The wild-type and mutant-expressing cells were left untreated, treated with LPS (1 μg/ml) for 15 min, or exposed to UV (60 J/m^2) for 2 h. The exogenous HA-tagged IκBα (exo IκBα) runs slightly higher than the endogenous IκBα (endo IκBα) due to the presence of the epitope tag.

indicated antibodies to evaluate the relative loading of both the kinase components and the substrate. Samples for coimmunoprecipitation experiments were resuspended in 10% PBS and 90% lysis buffer as described above except without the addition of phosphatase inhibitors. Immunoprecipitation samples were tumbled at 4°C overnight and washed five times with lysis buffer before Western blot analysis.

RESULTS

S32/36A mutant of IκBα prevents NF-κB activation by UV. While we were investigating the activation pathways induced by the topoisomerase inhibitors CPT and VP16, we began employing UV activation of NF-κB as a negative control due to the recent reports describing its involvement of a unique activation pathway (1, 21). We first examined the dose response and time course of NF-κB activation by UV by using EMSA. Exposure of HeLa cells to UV resulted in a time course and dose-dependent induction of NF-κB DNA-binding activity that

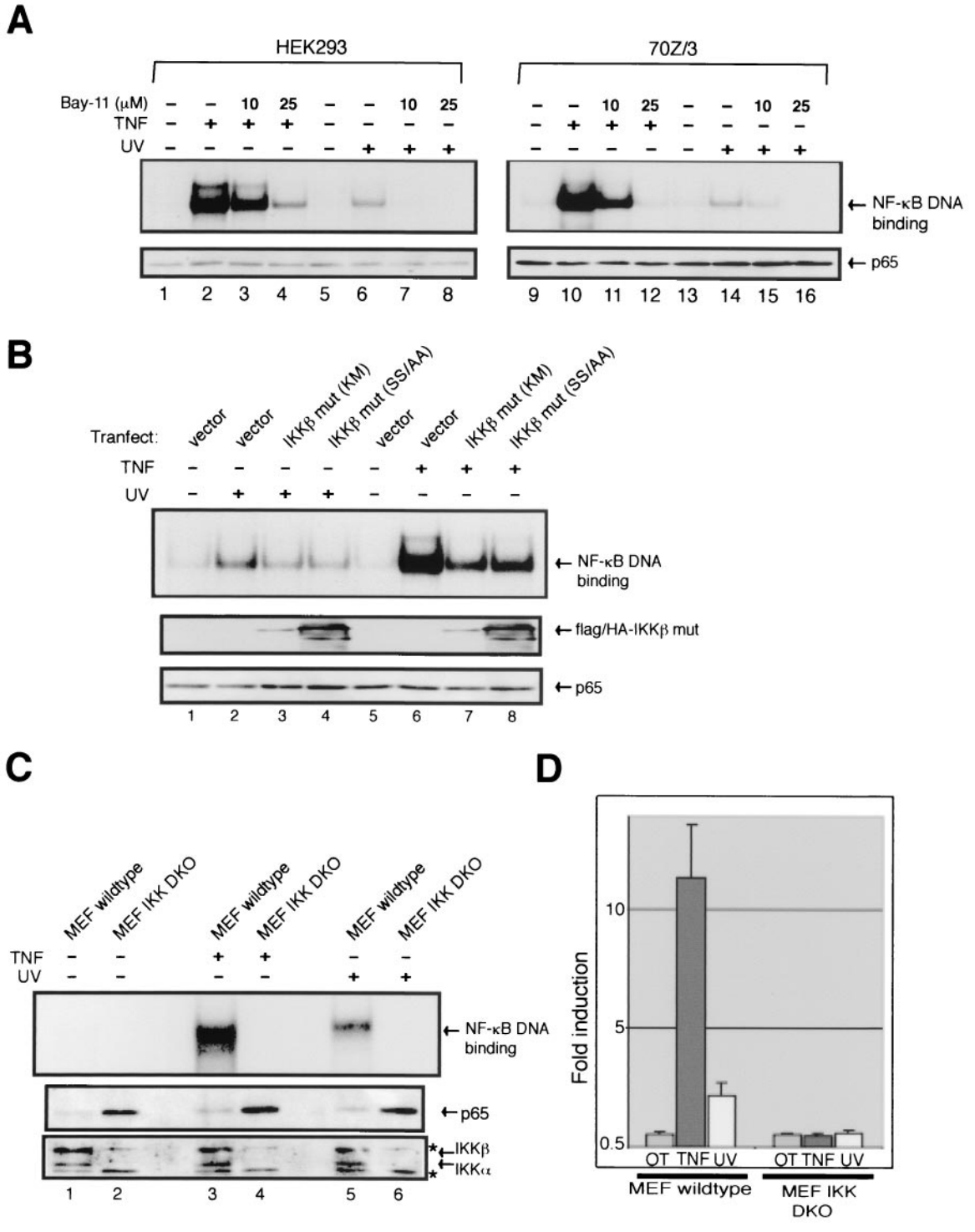

FIG. 2. IKK is required for UV-induced NF-κB activation. (A) HEK293 and 70Z/3 cells were both pretreated with 10 μM (lanes 3, 7, 11, and 15) or 25 μM (lanes 4, 8, 12, and 16) of the IKK inhibitor Bay-11-7082 and then treated with TNF-α (10 ng/ml) for 20 min in HEK293 or LPS (10 μg/ml) in 70Z/3 cells for 30 min as positive controls, or they were exposed to UV (60 J/m^2) irradiation for 2 h (70Z/3) or 4 h (HEK293) as indicated. Total cell extracts were made and analyzed by EMSA for NF-κB binding activity and Western blotting for p65 protein for a loading control. (B) HEK293 cells were transiently transfected with either vector control (1.0 μg), FLAG-tagged IKKβ mutant (Lys-to-Met mutation at the putative ATP-binding site; 1.0 μg), or HA-tagged IKKβ activation loop mutant (Ser177/181-to-Ala; 1.0 μg) as indicated. Cells were then either untreated or treated with TNF-α (10 ng/ml) or exposed to UV (60 J/m^2) for 4 h as indicated. Total cell extracts were made and analyzed by EMSA for NF-κB binding activity and Western blotting for Flag- and HA-tagged proteins in the same immunoblot with antibodies against both FLAG and HA or for p65 protein expression levels as indicated. The expression levels of IKKβ mut (SS/AA) appear higher possibly due to an efficient HA immunodetection. (C) MEF lines derived from wild-type or IKKα and IKKβ DKO MEFs were either left untreated, treated with TNF-α (10 ng/ml) for

was maximal in cells receiving 60 J of UV-C/m^2 for 2 h (Fig. 1A). In contrast, TNF-α-induced activation of NF-κB was more robust and peaked earlier at ca. 15 min (Fig. 1A and data not shown) (1). Consistent with previous findings (1, 21), similar UV dose response and time course of NF-κB activation were also observed in various cell types tested, including murine 70Z/3 pre-B cells.

Next, we examined the effect of UV on IKK activity. Proteins isolated at various intervals after exposure of 70Z/3 cells to UV were immunoprecipitated with an IKKα antibody and then subjected to an immunecomplex kinase assay by using GST-IκBα1-66 as a substrate. In agreement with an earlier report (21), UV had no measurable effect on IKK activity (Fig. 1B, lanes 6 and 9 to 12). IKK activity was detectable by two other "slow-kinetic" inducers (13), CPT and VP16 (Fig. 1B, lanes 3 and 4). LPS stimulation served as the positive control in these experiments (lanes 2 and 8).

Cytokine-inducible phosphorylation of IκBα at serines 32 and 36 is necessary for its degradation and subsequent NF-κB activation. We assessed whether UV-induced activation of NF-κB also required the IKK phospho-acceptor sites on IκBα. To examine this, we generated both N-terminally HA-tagged wild-type IκBα and an S32/36A IκBα mutant, in which serines 32 and 36 were replaced by alanines. These expression constructs were then stably introduced in 70Z/3-CD14 cells, and high expressing clones were isolated (13). Surprisingly, we found that the UV-induced NF-κB binding activity was completely inhibited in these mutant clones (Fig. 1C, lanes 4 to 6 [and others not shown]). Both LPS and UV induced NF-κB DNA-binding activity and degradation of IκBα in wild-type IκBα expressing clones (Fig. 1C, lanes 1 to 3). Although the induction of the IKK kinase activity was undetectable by the conventional in vitro immunecomplex kinase assay, these results indicate that the IKK phosphorylation sites on IκBα are required for the UV-induced activation of NF-κB in 70Z/3 cells.

IKK is involved in the UV-induced NF-κB activation pathway. Since the IKK phospho-acceptor sites of IκBα were required for UV-induced NF-κB activation, we examined by pharmacological and molecular methods whether the catalytic activity and components of the IKK complex were necessary for UV signaling. Consistent with an earlier report (28), the pretreatment of either HEK293 or 70Z/3 cells with the IKK chemical inhibitor Bay-11-7082 was able to dose dependently inhibit both TNF- and LPS-induced NF-κB binding activity as measured by EMSA (Fig. 2A). UV-induced NF-κB activation was also dose dependently inhibited by Bay-11 (Fig. 2A). This inhibitor did not directly affect NF-κB DNA-binding activity in vitro, whereas LPS-induced IκB kinase activity in 70Z/3 cells was blocked when the Bay-11 inhibitor was added directly in the in vitro kinase reaction (data not shown). Additionally, another unrelated IKK chemical inhibitor, 4-hydroxy-2-nonenal (HNE), also dose dependently reduced UV induction of NF-κB DNA-binding activity (data not shown) (16). Consistent with these observations, overexpression of a kinase inactive IKKβ(KM) mutant inhibited UV-induced NF-κB activation (Fig. 2B, compare lanes 2 and 3). The use of EMSA analysis to investigate potential inhibitory effects was possible because transfection efficiency of HEK293 cells was consistently >80%, and thus almost all cells in the transfected population expressed the IKKβ mutant proteins (13). Interestingly, the IKKβ(S177/181A) mutant in which the activation loop phosphorylation sites were mutated to alanines also reduced NF-κB activation by UV exposure (lane 4).

To further determine the necessity of the IκB kinases in NF-κB activation by UV, embryonic fibroblast lines derived from IKKα and IKKβ DKO mice were treated with TNF-α or UV. Consistent with published observations (22), TNF-α-induced activation of NF-κB was completely abolished in the IKK DKO MEFs (Fig. 2C). Similarly, NF-κB activation by UV exposure was undetectable in the DKO cells, even though activation was detectable in the parental wild-type line (Fig. 2C). Consistent with the EMSA findings, UV could not induce NF-κB-dependent transcriptional activation in the DKO MEFs, whereas UV generated a 2.5-fold NF-κB transcriptional induction as measured by the luciferase assay (Fig. 2D). These results together indicate that the catalytic activity and components of the IKK complex is crucial for NF-κB activation by UV.

Wild-type NEMO reconstitutes the UV-induced NF-κB signaling defect in 1.3E2 cells. Next, we assessed the requirement of NEMO, the regulatory component of IKK, for the activation of NF-κB by UV. The 1.3E2 cell line is a derivative of the 70Z/3 pre-B cell line that has lost the expression of NEMO (44). Consistent with the data above, UV could not activate NF-κB binding activity in the 1.3E2 cells (Fig. 3A, lanes 4 to 6). Unlike the targeted knockout cell systems described above for IKKα/IKKβ, the underlying reason for the NEMO deficiency in 1.3E2 cells is unclear. Thus, to prove that this UV defect in the latter cell system was indeed due to the lack of NEMO expression, wild-type Myc-tagged NEMO was stably introduced back into the 1.3E2 cells to determine whether the UV signaling pathway could be reconstituted. As expected, the LPS signaling defect in 1.3E2 cells can be efficiently reconstituted by the stable expression of wild-type NEMO (Fig. 3A, lane 8). Importantly, wild-type NEMO also efficiently complemented the UV-induced NF-κB signaling deficiency in 1.3E2 cells (Fig. 3A, lane 9). NF-κB activation by UV was much more robust than that seen in the parental cells (compare lanes 3 and 9), suggesting that NEMO levels likely represent a rate-limiting condition in the NF-κB signaling pathway induced by UV (compare NEMO levels between 70Z/3 and NEMO complemented 1.3E2 cells). Interestingly, even under the optimal condition for UV-induced activation of NF-κB, the in vitro immu-

15 min, or exposed to UV (60 J/m^2) irradiation for 2 h. Total cell extracts were made and analyzed by EMSA for NF-κB binding activity and Western blotting for IKKα, IKKβ and p65 protein expression as indicated. The asterisks indicate nonspecific bands. (D) Wild-type and DKO MEF lines were transiently transfected with an NF-κB-dependent reporter plasmid (3xκB-Luc) and an internal control for transfection efficiency (CMV-β-Gal). At 36 h after transfection, cells were either untreated or treated with TNF-α (10 ng/ml) or exposed to UV (60 J/m^2). Cell extracts were analyzed for luciferase and β-Galactosidase activities. Error bars indicate standard deviations. β-Galactosidase activities in DKO MEF were similar to those in wild-type MEF, indicating that the lack of luciferase induction in DKO cells was not due to inefficient transfection of these cells.

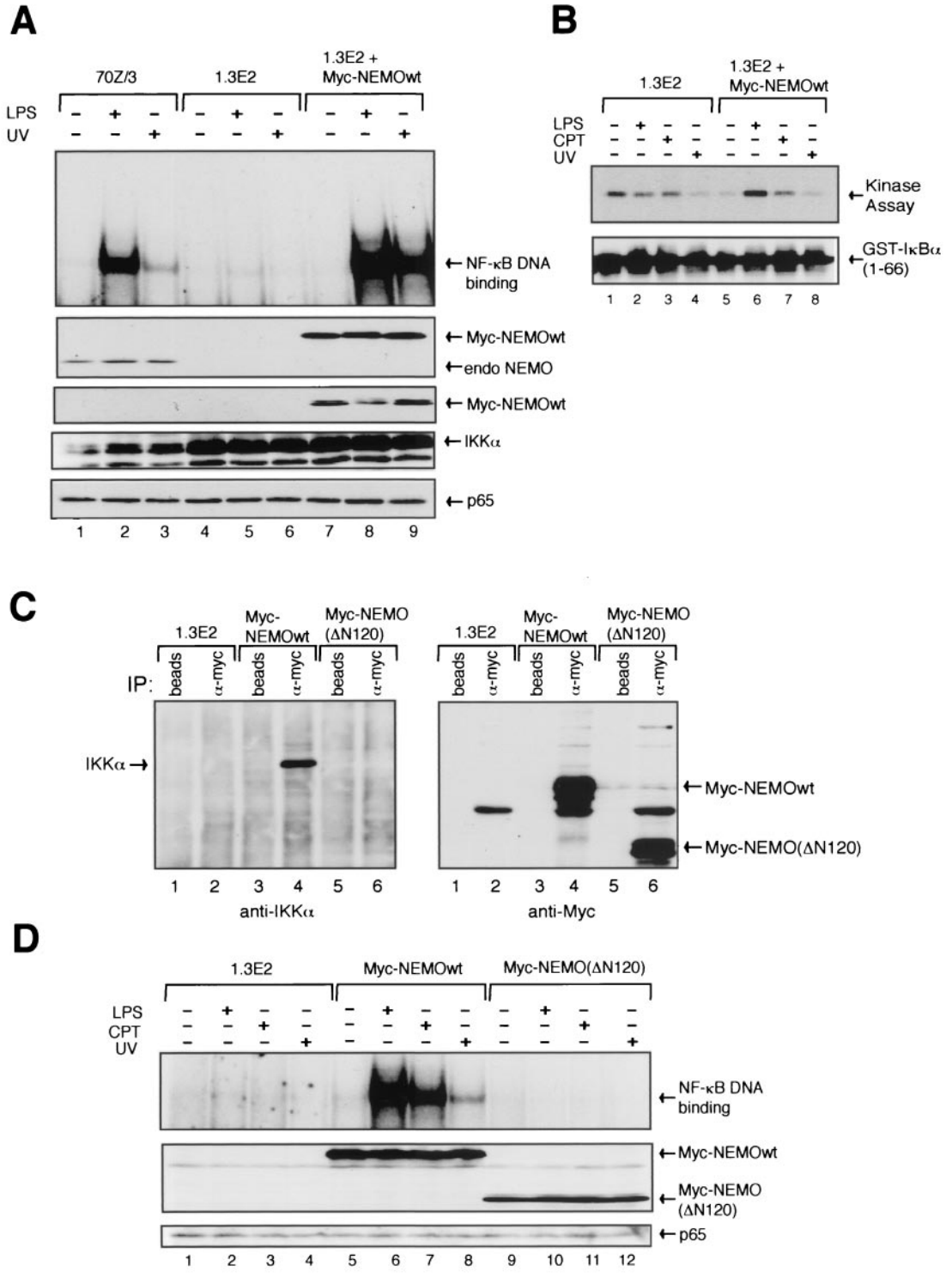

FIG. 3. NEMO association with the IKK catalytic core is necessary for UV-induced NF-κB activation. (A) A stably transfected pool of 1.3E2 cells expressing the Myc-tagged wild-type human NEMO, the NEMO-deficient 1.3E2 cells, and the 70Z/3 parental cells were either untreated or treated with LPS (10 μg/ml) for 30 min or exposed to UV (60 J/m^2) for 2 h and coanalyzed by EMSA and Western blotting (panels from top to bottom: antibodies against NEMO, c-Myc, IKKα, and p65) as indicated. (B) Myc-NEMO wild-type-expressing pool of 1.3E2 cells and the NEMO-deficient 1.3E2 cells were either untreated or treated with LPS (as described above), CPT (10 μM), or UV for 2 h. Whole-cell lysates were prepared and IKK activity was measured by the immune complex kinase assay (upper panel). Membrane was also immunoblotted with anti-GST antibody for loading control (lower panel). (C) Coimmunoprecipitation studies were done with 1.3E2 cells, Myc-NEMO wild-type-expressing 1.3E2 cells (D10 clone), and Myc-NEMO (ΔN120) cells. Extracts prepared from 10^7 cells per sample were immunoprecipitated with protein G-Sepharose beads only or with anti-c-Myc antibody overnight at 4°C. Samples were then loaded on an SDS-PAGE gel and examined by immunoblot with anti-IKKα and then anti-c-Myc antibodies as indicated. (D) A pool of 1.3E2 cells stably expressing an N-terminal 120-amino acid-truncated Myc-NEMO (ΔN120) was coanalyzed with 1.3E2 cells and the D10 Myc-NEMO wild-type-expressing 1.3E2 clone. Cells were either untreated or treated with LPS (10 μg/ml) for 30 min, CPT (10 μM) or UV (60 J/m^2) for 2 h. Total cell extracts were made and NF-κB binding activity was determined by EMSA. Protein expression levels of c-Myc-tagged proteins and p65 were also examined by Western blotting.

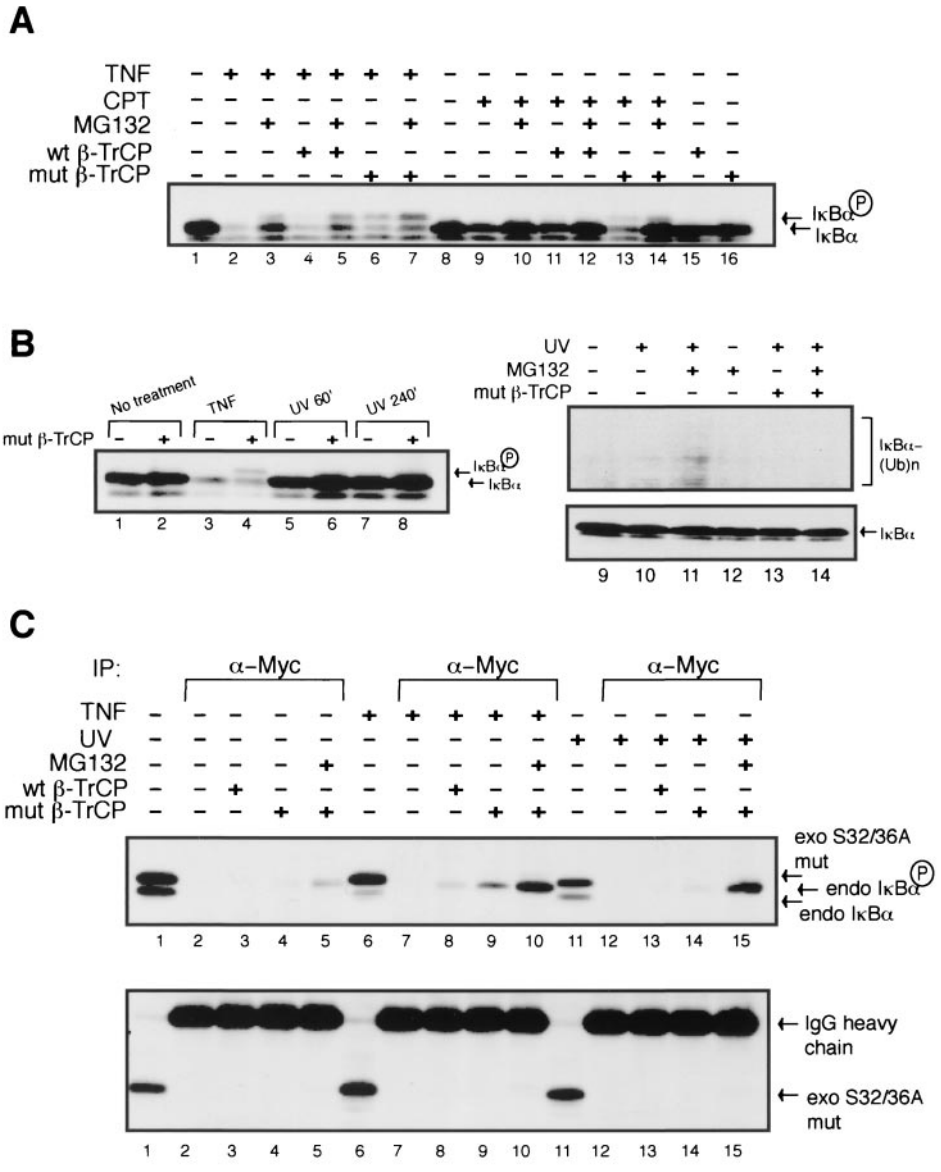

FIG. 4. UV-induced phosphorylation of IκBα is detectable by a ΔF-box mutant of β-TrCP as a specific phospho-protein substrate trap. (A) HEK293 cells were transiently transfected with either empty vector (1.0 μg), Myc-tagged wild-type β-TrCP (1.0 μg), or Myc-tagged ΔF-box β-TrCP (1.0 μg). At 36 h after transfection, cells were either left untreated or were treated with TNF-α (10 ng/ml) for 15 min or CPT (10 μM) for 2 h with or without pretreatment with MG132 (10 μM). Samples were then directly boiled in 2× SDS loading buffer prior to loading them on an SDS–12.5% PAGE gel. pIκBα migrated higher than the basal IκBα in a Western blot assay with an antibody against IκBα. (B) HEK293 cells were transiently transfected with empty vector or the ΔF-box mutant of β-TrCP and either left untreated or treated with TNF-α (as described above) or UV (60 J/m^2) at the indicated times or for 4 h in the presence of MG132 (as described above). Cell samples were analyzed as described above. The upper panel of lanes 9 to 14 represents a longer exposure of the upper regions of the immunoblot probed with the anti-IκBα antibody (lower panel). (C) A pool of HEK293 cells stably expressing HA-tagged S32/36A mutant of human IκBα were transiently transfected with either empty vector (1.0 μg), Myc-tagged wild-type β-TrCP (1.0 μg), or Myc-tagged ΔF-box β-TrCP (1.0 μg) as described above and treated as indicated. HEK293 cells were exposed to UV for 4 h for maximal NF-κB activation. A total of 5% of the extracts from untreated or treated samples was directly loaded to distinguish between the exogenous and endogenous IκBα proteins (lanes 1, 6, and 11). Samples were then collected, and cell lysates were made in a buffer containing phosphatase inhibitors (see Materials and Methods). The cell lysates were then subjected to coimmunoprecipitation with the anti-c-Myc antibody and immunoblotted for both endogenous and exogenous IκBα proteins (anti-IκBα antibody, top panel) or exogenous IκBα protein only (anti-HA antibody, bottom panel). Three IκBα forms can be detected (top panel). The lowest band corresponds to the basal endogenous IκBα. The middle band correlates to the endogenous pIκBα. The highest band represents the nondegradable exogenous HA-tagged S32/36A mutant IκBα.

necomplex kinase assay failed to detect any evidence of IKK activation (Fig. 3B, lane 8). The basal IKK activity in 1.3E2 was higher than that seen in the NEMO complemented cells (compare lanes 1 and 5). As expected, inducible IKK activation by both LPS and CPT was recovered in the complemented cells (lanes 6 and 7). Even though UV-induced IKK activation could not be readily detected by the in vitro kinase assay, these findings suggest that all of the core IKK

components are required for efficient activation of NF-κB by UV exposure.

To confirm that the requirement of NEMO in the UV signaling pathway is mechanistically linked to its direct function with the catalytic kinases IKKα and IKKβ, we generated an N-terminal 120-amino-acid deletion mutant of NEMO (ΔN120) that has been previously reported to be incapable of interacting with IKKα and IKKβ (24, 25, 31, 46). The NEMO (ΔN120) was stably expressed in 1.3E2 cells. Coimmunoprecipitation studies demonstrated that the stably expressed Myc-tagged wild-type NEMO in 1.3E2 cells could interact with IKKα by using a monoclonal antibody against c-Myc (Fig. 3C, left panel, lanes 3 and 4). Consistent with a previous report (46), the c-Myc antibody could not immunoprecipitate IKKα from Myc-tagged NEMO ΔN120-expressing 1.3E2 cells (Fig. 3C, left panel, lanes 5 and 6). The expression levels of Myc-NEMO wild type and ΔN120 were comparable, as shown by an anti-c-Myc immunoblot after coimmunoprecipitation (Fig. 3C, right panel, lanes 4 and 6). As expected, NF-κB inducers that have been previously characterized to involve IKK activation in their pathway, such as LPS and CPT, could not activate NF-κB binding activity in the Myc-tagged NEMO ΔN120-expressing 1.3E2 cells (Fig. 3D, lanes 9 to 11). Moreover, NEMO ΔN120 also failed to complement the NF-κB activation defect after UV exposure (lane 12). These results suggest that the interaction between NEMO and IKKα/IKKβ is essential for the UV-induced NF-κB activation pathway.

UV-inducible pIκBα is efficiently trapped by overexpression of an ΔF-box β-TrCP mutant. The results thus far strongly indicate that the IKK complex and its catalytic activity are directly involved in the UV-induced NF-κB signaling pathway. Moreover, stable expression of the S32/36A mutant of IκBα is effective at preventing NF-κB activation by UV. However, as was reported previously (21), we could not detect pIκBα after stimulation with UV. Likewise, a similar obstacle was encountered when we tried to characterize the DNA damage-induced NF-κB signaling pathway with CPT. We could show the genetic requirement of NEMO, IKKα, IKKβ, and the IKK phospho-acceptor sites of IκBα but failed to trap the pIκBα even in the presence of proteasome inhibitors after CPT treatment (13). It has been shown that overexpression of a ΔF-box mutant of β-TrCP in HEK293 cells can retard the ubiquitination and degradation of IκBα by TNF-α (36). We sought to determine whether this technique could also enhance the capture of pIκBα with slow-kinetic inducers such as CPT or UV.

The TNF-α-generated pIκBα is readily detected by Western blot analysis with pretreatment of HEK293 cells with the proteasome inhibitor MG132, followed by a 15-min TNF-α stimulation (Fig. 4A, lanes 1 to 3). This phospho-intermediate can be recapitulated by overexpressing Myc-tagged ΔF-box β-TrCP, followed by TNF-α induction (lane 6). Likewise, overexpression of ΔF-box β-TrCP, followed by stimulation with CPT, allowed for the detection of pIκBα (lane 13). The pIκBα indeed represented the same TNF-α-induced species seen by pretreatment with MG132. However, overexpression of Myc-tagged wild-type β-TrCP, followed by TNF-α or CPT treatment, does not trap pIκBα (lanes 4 and 11). As a control, neither the expression of wild-type β-TrCP nor that of ΔF-box β-TrCP was capable of capturing the pIκBα in the absence of stimulation (lanes 15 and 16). Curiously, unlike TNF-α, CPT-induced phosphorylation of IκBα could not be readily detected by MG132 pretreatment (lane 10). However, treatment of cells with proteasome inhibitor along with the expression of ΔF-box β-TrCP enhanced the capture of pIκBα induced by CPT (lane 14).

In contrast to our findings with TNF-α and CPT, we were unable to trap the pIκBα after UV exposure when we overexpressed ΔF-box β-TrCP in HEK293 cells, even in the presence of MG132 (Fig. 4B, compare lanes 5 to 8 and the lower panel of lanes 11 to 14). It was shown previously that UV-induced NF-κB activation was abolished in the temperature-sensitive ubiquitin-activating enzyme E1 *ts*20 cell line only at the restrictive temperature, suggesting that NF-κB activation by UV exposure requires ubiquitination of IκBα (21). Accordingly, we were able to detect multiubiquitinated IκBα after treatment with UV, particularly in the presence of MG132 (Fig. 4B, upper panel, lane 11), whose levels were reduced to undetectable levels by the expression of ΔF-box β-TrCP (upper panel of lane 14). To specifically capture the potentially labile pIκBα induced by UV exposure, we made the assay even more sensitive with built-in controls by first engineering HEK293 cells to stably express HA-tagged S32/36A IκBα, transiently transfected the cells with Myc-tagged wild-type or ΔF-box β-TrCP, and then treated them with TNF-α or UV in the presence or absence of proteasome inhibitors. The treated samples were then subjected to a coimmunoprecipitation step with the anti-c-Myc antibody to pull down pIκBα bound to β-TrCP. While very little endogenous pIκBα could be detected upon UV exposure in the presence of ΔF-box β-TrCP alone (Fig. 4C, top panel, lane 14), much more pIκBα was captured when MG132 pretreatment was added (top panel, lane 15). The pIκBα detection was not due to MG132 treatment alone since ΔF-box β-TrCP expression, followed by MG132 treatment, did not trap significant amount of the pIκBα intermediate (top panel, lane 5). Also, wild-type β-TrCP expression followed by MG132 treatment did not allow the detection of UV-induced pIκBα species (data not shown). The UV-induced interaction of pIκBα with mutant β-TrCP was dependent on phosphorylation of serines 32 and 36 since the HA-tagged S32/36A IκBα mutant could not be coimmunoprecipitated with the anti-c-Myc antibody under any of the treatment conditions (Fig. 4C, lower panel). Thus, by using a more sensitive strategy to trap the inducible pIκBα, UV exposure was found to induce the phosphorylation of IκBα on serines 32 and 36 in an IKK-dependent manner.

Mutations of the C-terminal zinc finger domain of NEMO abolish UV-induced NF-κB activation. It has been proposed that the IKK complex is the point of convergence for most NF-κB-activating stimuli and that NEMO might act as a molecular bridge to activate IKK (14). In order to determine which region(s) of NEMO is necessary for UV-induced NF-κB activation, Myc-tagged C-terminal deletion mutants of NEMO were made and stably expressed in 1.3E2 cells for analyses (data not shown). Surprisingly, we found that truncation of the last 25 amino acids of NEMO (ΔC25), which encodes a putative zinc finger domain, completely abolished UV-induced NF-κB binding activity (Fig. 5A, upper panel, compare lanes 5 and 10). Other slow-kinetic inducers, such as CPT and VP16, also failed to activate NF-κB in these cells (upper panel, lanes 3 and 4). However, unexpectedly, the LPS signaling pathway

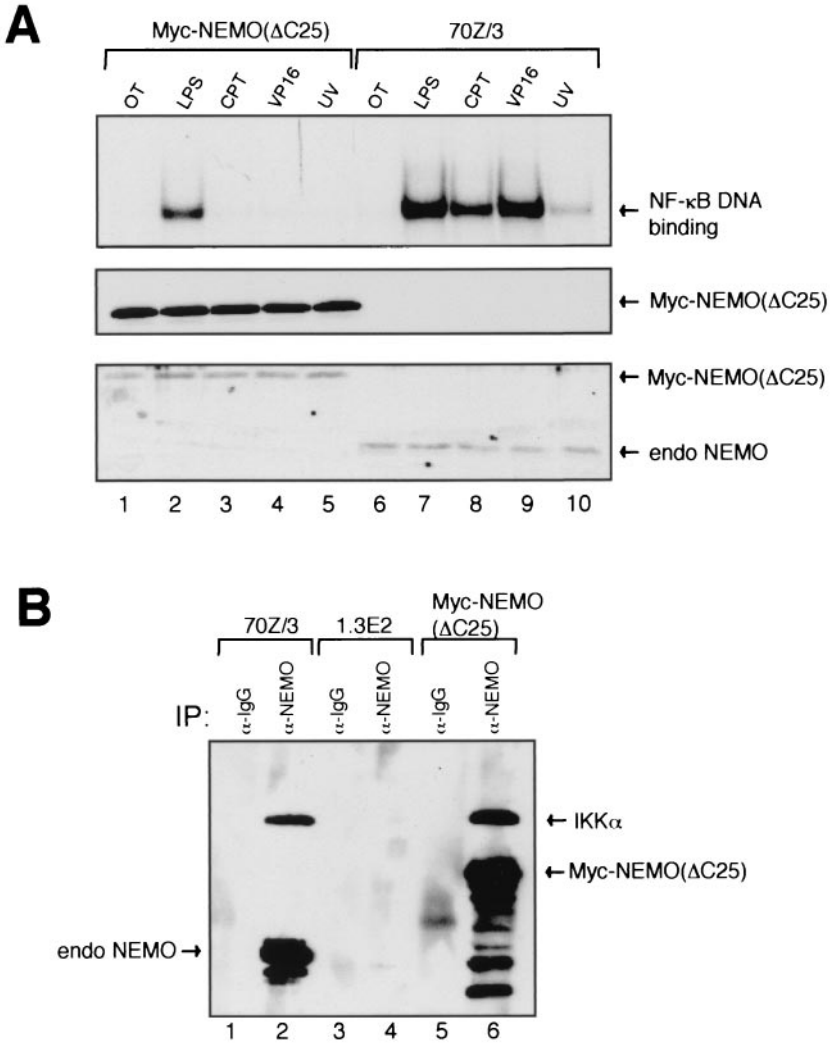

FIG. 5. UV-induced activation of NF-κB selectively requires the C-terminal 25 amino acids of NEMO. (A) 70Z/3, 1.3E2, and Myc-NEMO (ΔC25)-expressing 1.3E2 cells were treated as indicated, and the NF-κB binding activity was analyzed by EMSA (top panel), Myc-NEMO was detected in an immunoblot with an anti-c-Myc antibody (middle panel), and the relative expression levels of both Myc-NEMO (ΔC25) and wild-type endogenous NEMO were compared with a Western blot probed with anti-NEMO antibody (lower panel). (B) Coimmunoprecipitation studies were done with 70Z/3, 1.3E2, and Myc-NEMO (ΔC25)-expressing 1.3E2 cells. A total of 10^7 cells per sample were lysed and immunoprecipitated with either rabbit immunoglobulin G or anti-NEMO antibodies. The samples were subjected to SDS-PAGE and then immunoblotted with anti-IKKα and -NEMO antibodies.

was still intact in the 1.3E2 cells expressing NEMO ΔC25 (upper panel, lane 2). The expression level of exogenous NEMO ΔC25 in 1.3E2 cells was comparable to that of endogenous NEMO in 70Z/3 cells (lower panel). Coimmunoprecipitation studies showed that NEMO ΔC25 also interacted with IKKα at similar levels to that of wild-type NEMO (Fig. 5B).

The last 25 amino acids of NEMO encode a putative zinc finger domain (Fig. 6A). While our study was ongoing, a report was published regarding the identification of specific missense mutations in the putative zinc finger domain of NEMO in a human disease called X-linked primary immunodeficiency, characterized by hyper-immunoglobulin M syndrome and hypohydrotic ectodermal dysplasia (XHM-ED) (15). The mutations result in codon changes of cysteine 417 to arginine and aspartic acid 406 to valine in the C-terminal region (Fig. 6A). Analysis of the cells derived from the affected patients showed that NF-κB activation was intact after treatments with LPS or TNF-α but not with CD40L (15). To determine whether the lack of UV activation of NF-κB observed in 1.3E2 cells expressing NEMO ΔC25 was due to the lack of the zinc finger motif, the above natural zinc finger mutations in NEMO were examined for their effect on UV-induced activation of NF-κB. We first constructed NEMO point mutants, C417R, C417A, and D406V, and stably expressed them in 1.3E2 cells as described above. These reconstitution experiments demonstrated that the LPS-induced NF-κB activation was only modestly affected by C417R, C417A, and D406V point mutations (Fig. 6B, lanes 2, 8, 11, and 14). However, the point mutations in the zinc finger region of NEMO completely prevented UV-induced

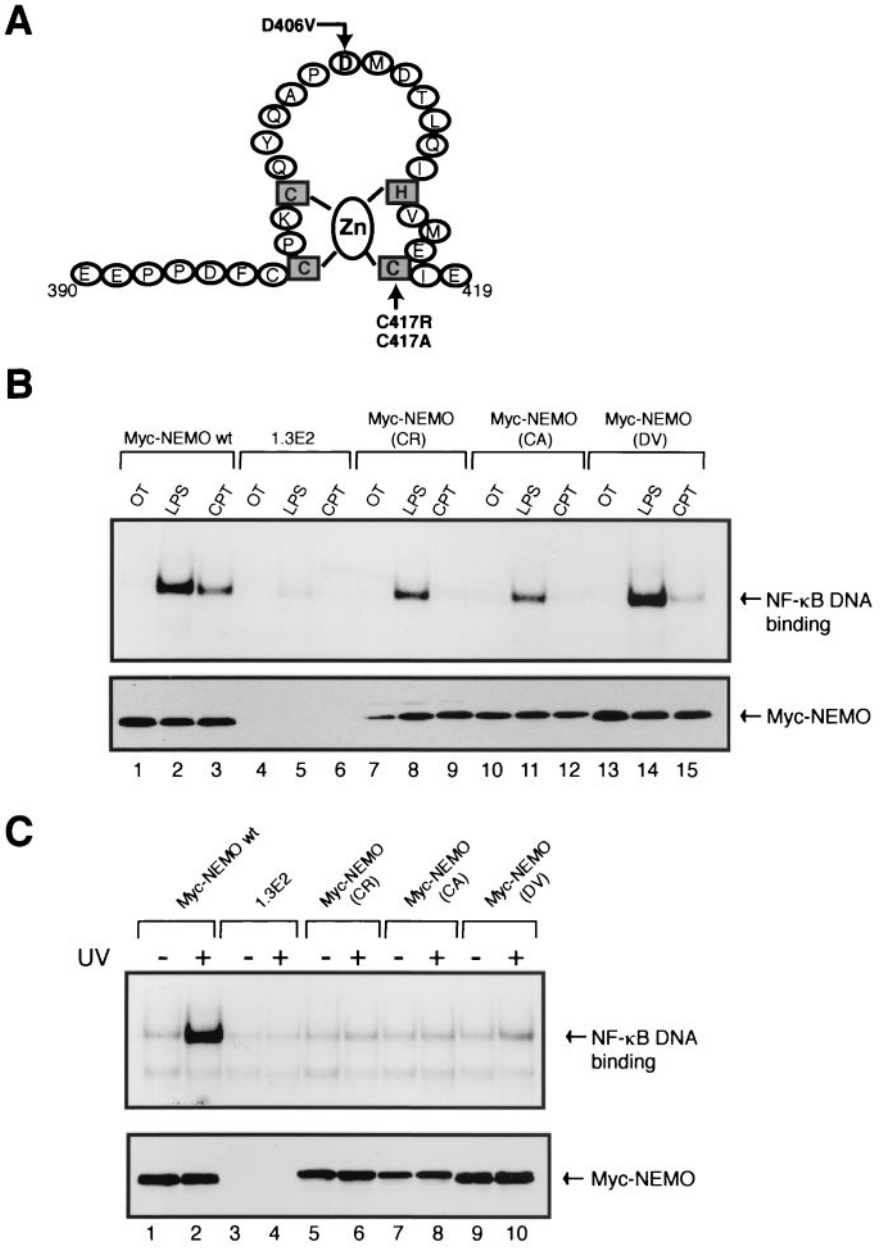

FIG. 6. NEMO zinc finger point mutations greatly compromise the ability of the cells to activate NF-κB by UV and topoisomerase inhibitors. (A) Diagram depicting point mutations in the $Cys_2HisCys$ zinc finger region generated and analyzed in this study. (B) The two known naturally occurring point mutations in the putative zinc finger domain of NEMO (C417R and D406V) were generated as Myc-NEMO (CR) and Myc-NEMO (DV), respectively. Cysteine 417 was also changed to alanine and constructed as Myc-NEMO (CA). The three NEMO point mutants were stably expressed in 1.3E2 cells and analyzed, along with the Myc-NEMO wild-type-expressing 1.3E2 clone D10 and the parental 1.3E2 cells. The five different cell lines were either left untreated or treated with LPS (10 μg/ml) for 30 min or with CPT (10 μM) for 2 h. Total cell extracts were made and analyzed by EMSA for NF-κB binding activity (upper panel) and by Western blotting (anti-c-Myc antibody) for protein expression levels of the Myc-tagged NEMO wild-type and point mutants (lower panel). (C) The five cell lines were also exposed to UV (60 J/m^2) for 2 h and analyzed by EMSA (upper panel) and Western blot assay (lower panel) as described above.

NF-κB activation (Fig. 6C). This was also the case for two other slow-kinetic inducers, CPT (Fig. 6B) and VP16 (data not shown). These results demonstrate that the putative zinc finger domain at the C-terminal region of NEMO is essential for UV-induced activation of NF-κB. Moreover, this zinc finger region appears to be selectively required for signaling pathways initiated by relatively slower and/or weaker NF-κB-activating conditions.

DISCUSSION

Earlier studies have proposed that the signaling event through which UV triggers the degradation of IκBα to be distinct from that of the cytokine-induced signaling pathway (1, 21). Here we provide evidence that the IκB kinases and the regulatory subunit, NEMO, are indeed necessary components

in the UV-induced NF-κB signaling pathway. NEMO-deficient or IKKα and IKKβ doubly deficient cell lines fail to increase NF-κB DNA-binding activity upon UV exposure in comparison to their wild-type counterparts. Moreover, replacing the IKK phospho-acceptor sites of IκBα, serines 32 and 36, with nonphosphorylatable alanine residues not only prevents its inducible degradation by UV but also abolishes NF-κB activation after UV treatment. To determine whether these sites were inducibly phosphorylated by UV, we developed a very sensitive strategy to capture the pIκBα. Using the dominant-negative mutant form of the receptor subunit of the SCF ubiquitin ligase β-TrCP as bait, we were able to efficiently trap the UV-inducible pIκBα intermediate. These results suggest that the UV pathway utilizes IKK to phosphorylate IκBα and target it for proteolysis by a β-TrCP-dependent ubiquitin proteasome pathway.

Several inconsistencies, however, still loom over the mechanism involved in the UV-induced NF-κB signaling pathway. First, although both the components and the catalytic activity of the IKK complex were found to be required for UV-induced NF-κB binding activity in the present study, the detection of an increase in the IKK kinase activity remains elusive. Consistent with the previous report by Li and Karin (21), we also failed to detect any evidence of the increase in IKK activity after exposure of different cells to various doses and time durations of UV exposure. The IKK activity, as measured by the in vitro immunecomplex kinase assay, is not detectably elevated above the basal level IKK activity, even though it reproducibly dips below the unstimulated levels at ca. 60 min and returns to basal levels after 90 min of UV exposure (T. T. Huang, unpublished data). It is unclear whether the inability to detect IKK activation is due to some deficiency of the in vitro assay to truly recapitulate in vivo activation of this kinase complex after UV stimulation or whether it is due to the presence of an IKK-inactivating phosphatase(s) which prevents the detection of possible UV-induced IKK activation. Rapid activation of a PP2A-like protein phosphatase has been observed after UV irradiation in NIH 3T3 cells (41), and PP2A has been implicated in the regulation of IKK activation (3, 7). Alternatively, the basal IKK activity may be all that is necessary to phosphorylate IκBα in response to UV stimulus without any "induction" of its kinase activity. Significantly, however, the dual mutations of the phosphorylation sites within the activation loop of IKKβ interfered with UV activation of NF-κB under our experimental conditions, suggesting that inducible phosphorylation of IKKβ at these sites is likely necessary for this UV pathway as for the cytokine-inducible pathways (5).

Second, other groups have previously suggested that the IKK phospho-acceptor sites on IκBα are not required for UV-induced IκBα degradation. These experiments were done either by the analysis of transiently transfected IκBα wild type or S32/36A mutant in HeLa cells, followed by UV stimulation (1), or by analysis of pools of stably transfected HeLa cells expressing either wild-type or S32/36A mutant IκBα (21). In both cases, the expression levels of the mutant IκBα were comparably lower than were the endogenous IκBα levels. It was not known whether their expression of the mutant IκBα could inhibit UV-induced NF-κB activation, since its effect on NF-κB DNA-binding activity was not reported in these previous studies. We found that in the 70Z/3 cell background, the mutant IκBα clearly blocked NF-κB activation by UV exposure. In addition, we found that UV exposure enhanced caspase-mediated cleavage of IκBα, independent of serines 32 and 36, at longer time points (data not shown). Pretreatment of 70Z/3 cells with a pan-caspase inhibitor, such as z-VAD, was required to blocked the minor degradation of S32/36A mutant IκBα. Nevertheless, UV-induced activation of NF-κB, as measured by EMSA, was completely blocked in S32/36A mutant-expressing cells, even without the presence of caspase inhibitors. Such parallel effects of UV might have contributed, in part, to the degradation of S32/36A mutant of IκBα at longer time points after UV exposures. It is also possible that different cell types may elicit distinct mechanisms of NF-κB activation by UV.

Many previous studies on the mammalian UV response primarily focused on the activation of AP-1 as one key endpoint (6, 19, 30, 33). It has been shown that UV irradiation can stimulate the activity of a variety of mitogen-activated protein kinases, including JNK, p38, and ERK, and can therefore induce the subsequent phosphorylation of transcription factors, such as c-Jun, ATF-2, and Elk-1 (17). It was suggested that UV exposure activates cell surface receptors, such as the epidermal growth factor and TNF receptors, in ligand-independent fashions to activate mitogen-activated protein kinases (30, 33, 39). Two mechanisms have been proposed to explain the activation of cell surface receptors by UV: (i) UV-induced receptor clustering (30) and (ii) inhibition of receptor-inactivating protein phosphatases (19). Thus, by mimicking the action of growth factors and cytokines, UV irradiation may activate signaling pathways that lead to the induction of NF-κB activity.

Consistent with this notion, we found that many of the downstream signaling events, which lead to the degradation of IκBα and NF-κB activation by UV, are surprisingly parallel to those induced by cytokine or other cell surface receptors, such as that for LPS and TNF-α. However, how the initial UV signal, generated at the cell surface by a ligand-independent mechanism, can communicate with the IKK complex is not clear. Even though the components involved are similar, our findings suggest that ligand-induced signals and those induced by UV are processed somewhat differently and likely evoke distinct reactions on the IKK complex. We found an intriguing observation that the C-terminal zinc finger domain of NEMO, when in complex with the catalytic kinases, is essential for UV-induced NF-κB activation. However, unexpectedly, this region of NEMO is largely dispensable for LPS-dependent activation of NF-κB even though downstream events that target the degradation of IκBα appears to be the same. Recent studies by Jain et al. (15) showed that cells isolated from patients with XHM-ED contain mutations in the NEMO zinc finger region. The TNF-α- and LPS-induced NF-κB signaling pathways also appeared to be normal in cells from the affected patients. Thus, while the IKK-dependent downstream events are similar, UV activation of NF-κB invokes IKK regulation distinct from that induced by the classical cytokine pathways by means of the C-terminal NEMO zinc finger.

Interestingly, we found that the C-terminal NEMO zinc finger is also necessary for NF-κB activation by other relatively slower and weaker activators, such as CPT and VP16. These topoisomerase inhibitors activate NF-κB by causing IκBα degradation by mechanisms similar to those induced by cyto-

kines. Jain et al. (15) also showed that CD40L signaling to NF-κB was disrupted in the NEMO zinc finger mutant cells. This allowed us to categorize certain NF-κB inducers (CD40L, UV, CPT, and VP16) together that are highly sensitive to the disruption of the zinc finger structure of NEMO and group other NF-κB inducers (TNF-α and LPS) that are not as sensitive. Since maximal activation of NF-κB by UV, CPT, and VP16 is generally weaker and reach peak activation at much slower kinetics than do cytokines and LPS, IKK activation processes that occur under these different conditions may be different. It is possible that the putative zinc finger module of NEMO is a protein interaction domain that recruits other cofactors necessary for a specific subset of NF-κB inducers. Alternatively, mutations in the zinc finger region could alter the integrity of other possible protein-protein interaction domains in NEMO or in IKKα/β complexes. Strong and rapid activators of NF-κB may bypass the requirement of these interacting events involving the NEMO zinc finger region to induce IKK, whereas weaker and slower activators may heavily depend on these interactions. Thus, we propose that a hallmark for slow-kinetic and weak IKK-dependent NF-κB inducers may be the critical involvement of the zinc finger domain of NEMO to modulate IKK activity. Finding the mechanism by which the NEMO zinc finger contributes to select IKK activation events may provide a useful target to selectively modulate a set of NF-κB-dependent processes to treat human diseases, such as cancer and XHM-ED.

ACKNOWLEDGMENTS

We thank I. Verma for wild-type and IKK1/α and IKK2/β DKO MEF lines, A. Israel for 1.3E2 cells, Z. Chen for Myc-tagged β-TrCP and NEMO expression constructs, M. Karin for IKKβ dominant-negative mutant constructs, B. Seufzer and S. Shumway for technical support, and the Miyamoto lab members for helpful discussions.

This work was supported in part by the Herman I. Shapiro Fellowship through the University of Wisconsin Medical School to T.T.H., by NIH grants R01-CA77474 and R01-CA81065, by a Howard Hughes Medical Institute fund through the University of Wisconsin Medical School, and by the Shaw Scientist Award from the Milwaukee Foundation to S.M.

REFERENCES

1. **Bender, K., M. Gottlicher, S. Witeside, H. J. Rahmsdorf, and P. Herrlich.** 1998. Sequential DNA damage-independent and -dependent activation of NF-κB by UV. EMBO J. **17:**5170–5181.
2. **Cao, Z. D., J. Xiong, M. Takeuchi, T. Kurama, and D. V. Goeddel.** 1996. TRAF6 is a signal transducer for interleukin-1. Nature **383:**443–446.
3. **Chen, Z., J. Hagler, V. J. Palombella, F. Melandri, D. Scherer, D. Ballard, and T. Maniatis.** 1995. Signal-induced site-specific phosphorylation targets IκBα to the ubiquitin-proteasome pathway. Genes Dev. **9:**1586–1597.
4. **Chen, Z. J., L. Parent, and T. Maniatis.** 1996. Site-specific phosphorylation of IκBα by a novel ubiquitination-dependent protein kinase activity. Cell **84:**853–862.
5. **Delhase, M., M. Hayakawa, Y. Chen, and M. Karin.** 1999. Positive and negative regulation of IκB kinase activity through IKKβ subunit phosphorylation. Science **284:**309–313.
6. **Devary, Y., R. A. Gottlieb, T. Smeal, and M. Karin.** 1992. The mammalian ultraviolet response is triggered by activation of Src tyrosine kinases. Cell **71:**1081–1091.
7. **DiDonato, J. A., M. Hayakawa, D. M. Rothwarf, E. Zandi, and M. Karin.** 1997. A cytokine-responsive IκB kinase that activates the transcription factor NF-κB. Nature **388:**548–554.
8. **Fuchs, S. Y., A. Chen, Y. Xiong, Z. Q. Pan, and Z. Ronai.** 1999. HOS, a human homolog of Slimb, forms an SCF complex with Skp1 and Cullin1 and targets the phosphorylation-dependent degradation of IκB and beta-catenin. Oncogene **18:**2039–2046.
9. **Ghosh, S., M. J. May, and E. B. Kopp.** 1998. NF-κB and Rel proteins: evolutionarily conserved mediators of immune responses. Annu. Rev. Immunol. **16:**225–260.
10. **Hatakeyama, S., M. Kitagawa, K. Nakayama, M. Shirane, M. Matsumoto, K. Hattori, H. Higashi, H. Nakano, K. Okumura, K. Onoe, and R. A. Good.** 1999. Ubiquitin-dependent degradation of IκBα is mediated by a ubiquitin ligase Skp1/Cul 1/F-box protein FWD1. Proc. Natl. Acad. Sci. USA **96:**3859–3863.
11. **Huang, T. T., N. Kudo, M. Yoshida, and S. Miyamoto.** 2000. A nuclear export signal in the N-terminal regulatory domain of IκBα controls cytoplasmic localization of inactive NF-κB/IκBα complexes. Proc. Natl. Acad. Sci. USA **97:**1014–1019.
12. **Huang, T. T., and S. Miyamoto.** 2001. Postrepression activation of NF-κB requires the amino-terminal nuclear export signal specific to IκBα. Mol. Cell. Biol. **21:**4737–4747.
13. **Huang, T. T., S. M. Wuerzberger-Davis, B. J. Seufzer, S. D. Shumway, T. Kurama, D. A. Boothman, and S. Miyamoto.** 2000. NF-κB activation by camptothecin: a linkage between nuclear DNA damage and cytoplasmic signaling events. J. Biol. Chem. **275:**9501–9509.
14. **Israel, A.** 2000. The IKK complex: an integrator of all signals that activate NF-κB? Trends Cell Biol. **10:**129–133.
15. **Jain, A., C. A. Ma, S. Liu, M. Brown, J. Cohen, and W. Strober.** 2001. Specific missense mutations in NEMO result in hyper-IgM syndrome with hypohydrotic ectodermal dysplasia. Nat. Immunol. **2:**223–228.
16. **Ji, C., K. R. Kozak, and L. J. Marnett.** 2001. IκB kinase, a molecular target for inhibition by 4-hydroxy-2-nonenal. J. Biol. Chem. **276:**18223–18228.
17. **Karin, M.** 1995. The regulation of AP-1 activity by mitogen-activated protein kinases. J. Biol. Chem. **270:**16483–16486.
18. **Karin, M., and Y. Ben-Neriah.** 2000. Phosphorylation meets ubiquitination: the control of NF-κB activity. Annu. Rev. Immunol. **18:**621–663.
19. **Knebel, A., H. J. Rahmsdorf, A. Ullrich, and P. Herrlich.** 1996. Dephosphorylation of receptor tyrosine kinases as target of regulation by radiation, oxidants or alkylating agents. EMBO J. **15:**5314–5325.
20. **Kroll, M., F. Margottin, A. Kohl, P. Renard, H. Durand, J. P. Concordet, F. Bachelerie, F. Arenzana-Seisdedos, and R. Benarous.** 1999. Inducible degradation of IκBα by the proteasome requires interaction with the F-box protein h-βTrCP. J. Biol. Chem. **274:**7941–7945.
21. **Li, N., and M. Karin.** 1998. Ionizing radiation and short wavelength UV activate NF-κB through two distinct mechanisms. Proc. Natl. Acad. Sci. USA **95:**13012–13017.
22. **Li, Q., G. Estepa, S. Memet, A. Israel, and I. M. Verma.** 2000. Complete lack of NF-κB activity in IKK1 and IKK2 double-deficient mice: additional defect in neurulation. Genes Dev. **14:**1729–1733.
23. **Malek, S., Y. Chen, T. Huxford, and G. Ghosh.** 2001. IκBβ, but not IκBα, functions as a classical cytoplasmic inhibitor of NF-κB dimers by masking both NF-κB nuclear localization sequences in resting cells. J. Biol. Chem. **276:**45225–45235.
24. **May, M. J., F. D'Acquisto, L. A. Madge, J. Glockner, J. S. Pober, and S. Ghosh.** 2000. Selective inhibition of NF-κB activation by a peptide that blocks the interaction of NEMO with the IκB kinase complex. Science **289:**1550–1554.
25. **Mercurio, F., B. W. Murray, A. Shevchenko, B. L. Bennett, D. B. Young, J. W. Li, G. Pascual, A. Motiwala, H. Zhu, M. Mann, and A. M. Manning.** 1999. IκB kinase (IKK)-associated protein 1, a common component of the heterogeneous IKK complex. Mol. Cell. Biol. **19:**1526–1538.
26. **Mercurio, F., H. Zhu, B. W. Murray, A. Shevchenko, B. L. Bennett, J. W. Li, D. B. Young, M. Barbosa, M. Mann, A. Manning, and A. Rao.** 1997. IKK-1 and IKK-2: cytokine-activated IκB kinases essential for NF-κB activation. Science **278:**860–866.
27. **Miyamoto, S., B. Seufzer, and S. Shumway.** 1998. Novel IκBα degradation process in WEHI231 murine immature B cells. Mol. Cell. Biol. **18:**19–29.
28. **Pierce, J. W., R. Schoenleber, G. Jesmok, J. Best, S. A. Moore, T. Collins, and M. E. Gerritsen.** 1997. Novel inhibitors of cytokine-induced IkappaBalpha phosphorylation and endothelial cell adhesion molecule expression show anti-inflammatory effects in vivo. J. Biol. Chem. **272:**21096–21103.
29. **Prigent, M., I. Barlat, H. Langen, and C. Dargemont.** 2000. IκBα and IκBα/NF-κB complexes are retained in the cytoplasm through interaction with a novel partner, RasGAP SH3-binding protein 2. J. Biol. Chem. **275:**36441–36449.
30. **Rosette, C., and M. Karin.** 1996. Ultraviolet light and osmotic stress: activation of the JNK cascade through multiple growth factor and cytokine receptors. Science **274:**1194–1197.
31. **Rothwarf, D. M., E. Zandi, G. Natoli, and M. Karin.** 1998. IKKγ is an essential regulatory subunit of the IκB kinase complex. Nature **395:**297–300.
32. **Rudolph, D., W. C. Yeh, A. Wakeham, B. Rudolph, D. Nallainathan, J. Potter, A. J. Elia, and T. W. Mak.** 2000. Severe liver degeneration and lack of NF-κB activation in NEMO/IKKγ-deficient mice. Genes Dev. **14:**854–862.
33. **Sachsenmaier, C., A. Radler-Pohl, R. Zinck, A. Nordheim, P. Herrlich, and H. J. Rahmsdorf.** 1994. Involvement of growth factor receptors in the mammalian UVC response. Cell **78:**963–972.
34. **Schmidt-Supprian, M., W. Bloch, G. Courtois, K. Addicks, A. Israel, K. Rajewsky, and M. Pasparakis.** 2000. NEMO/IKKγ-deficient mice model incontinentia pigmenti. Mol. Cell **5:**981–992.
35. **Silverman, N., and T. Maniatis.** 2001. NF-κB signaling pathways in mammalian and insect innate immunity. Genes Dev. **15:**2321–2342.

36. **Spencer, E., J. Jiang, and Z. J. Chen.** 1999. Signal-induced ubiquitination of IκBα by the F-box protein Slimb/β-TrCP. Genes Dev. **13:**284–294.
37. **Suzuki, H., T. Chiba, M. Kobayashi, M. Takeuchi, T. Suzuki, A. Ichiyama, T. Ikenoue, M. Omata, K. Furuichi, and K. Tanaka.** 1999. IκBα ubiquitination is catalyzed by an SCF-like complex containing Skp1, cullin-1, and two F-box/WD40-repeat proteins, betaTrCP1 and betaTrCP2. Biochem. Biophys. Res. Commun. **256:**127–132.
38. **Tam, W. F., and R. Sen.** 2001. IκB family members function by different mechanisms. J. Biol. Chem. **276:**7701–7704.
39. **Tobin, D., M. van Hogerlinden, and R. Toftgard.** 1998. UVB-induced association of tumor necrosis factor (TNF) receptor 1/TNF receptor-associated factor-2 mediates activation of Rel proteins. Proc. Natl. Acad. Sci. USA **95:**565–569.
40. **Verma, I. M., J. K. Stevenson, E. M. Schwarz, D. Van Antwerp, and S. Miyamoto.** 1995. Rel/NF-κB/IκB family: intimate tales of association and dissociation. Genes Dev. **9:**2723–2735.
41. **Voorhoeve, P. M., R. J. Watson, P. G. Farlie, R. Bernards, and E. W. Lam.** 1999. Rapid dephosphorylation of p107 following UV irradiation. Oncogene **18:**679–688.
42. **Winston, J. T., P. Strack, P. Beer-Romero, C. Y. Chu, S. J. Elledge, and J. W. Harper.** 1999. The SCFβ-TRCP-ubiquitin ligase complex associates specifically with phosphorylated destruction motifs in IκBα and beta-catenin and stimulates IκBα ubiquitination in vitro. Genes Dev. **13:**270–283.
43. **Woronicz, J. D., X. Gao, Z. Cao, M. Rothe, and D. V. Goeddel.** 1997. IκB kinase-β: NF-κB activation and complex formation with IκB kinase-α and NIK. Science **278:**866–869.
44. **Yamaoka, S., G. Courtois, C. Bessia, S. T. Whiteside, R. Weil, F. Agou, H. E. Kirk, R. J. Kay, and A. Israel.** 1998. Complementation cloning of NEMO, a component of the IκB kinase complex essential for NF-κB activation. Cell **93:**1231–1240.
45. **Yaron, A., A. Hatzubai, M. Davis, I. Lavon, S. Amit, A. M. Manning, J. S. Andersen, M. Mann, F. Mercurio, and Y. Ben-Neriah.** 1998. Identification of the receptor component of the IκBα-ubiquitin ligase. Nature **396:**590–594.
46. **Ye, J., X. Xie, L. Tarassishin, and M. S. Horwitz.** 2000. Regulation of the NF-κB activation pathway by isolated domains of FIP3/IKKγ, a component of the IκB-α kinase complex. J. Biol. Chem. **275:**9882–9889.
47. **Zandi, E., D. M. Rothwarf, M. Delhase, M. Hayakawa, and M. Karin.** 1997. The IκB kinase complex (IKK) contains two kinase subunits, IKKα and IKKβ, necessary for IκB phosphorylation and NF-κB activation. Cell **91:** 243–252.